HEFAT2012
9th International Conference on Heat Transfer, Fluid Mechanics and Thermodynamics
16 – 18 July 2012
Malta

EXPERIMENTAL STUDY ON THE HEAT TRANSFER IN SMALL CYCLONES

Sagot B.[1*] and Buron F.[2]
*Author for correspondence

[1]Laboratoire Fluide et Energétique,
Ecole Supérieure des Techniques Aéronautiques et Construction Automobile (ESTACA),
34 rue Victor Hugo - 92532 Levallois-Perret CEDEX, France

[2]Ecole d'Ingénieurs en Génie des Systèmes Industriels (EIGSI),
26 rue Vaux de Foletier - 17041 La Rochelle cedex 1, France
E-mail: benoit.sagot@estaca.fr

ABSTRACT

Cyclone separators are widely used in automotive applications, for the cleaning of hot oil mist. Most of the available studies are dealing with the cyclone collection efficiency, and the corresponding pressure drop. The aim of this experimental study is to investigate the gas-to-wall heat transfer, for a flow in a constant wall temperature cyclone configuration, to derive an average Nusselt number correlation. The cyclone is placed in a cold jacket, where the temperature is imposed by external circulation of a coolant. The simultaneous measurements of mass flow rate and characteristic temperatures (cyclone inlet, cold wall and cyclone outlet temperatures) permit the determination of the average wall heat transfer coefficient, through an enthalpy balance. Static pressure measurements at the inlet and outlet of the cyclone are used to evaluate the pressure drop in the cyclone, and a comparison between these results and those obtained by application of the currently available models. The inlet Reynolds number and geometry of the cyclone are varied. An average Nusselt number correlation is proposed for heat transfer in a cyclone under constant wall temperature conditions, as a function of the inlet Reynolds number Re_i ($400 \leq Re_i \leq 20\ 000$), and for different values of the dimensionless geometrical parameters L* ($0.75 \leq L^* \leq 2.5$).

INTRODUCTION

Cyclone separators are widely used in industrial applications for separating dispersed particles from their carrying gas. Theses devices are frequently used in large-scale processes, for both separation and drying applications. However, small cyclones have also found various applications, such as personal cyclone samplers used in environment control. Small cyclones are also widely used in the automotive industry, for the separation of oil mist from blow-by gases in combustion engines. Theses so-called "blow-by gases" result from combustion gas leakages between the combustion chamber and the crankcase, especially when piston rings wear occurs. One of the main purpose of crankcase venting systems is the separation of the oil mist resulting from the circulation of these blow-by gases through the crankcase, which contains lubricating oil. The diameter of the sampling cyclone is of great importance for its collection efficiency: a reduction of this size produces an increase of the collected oil flow, but also results in an increase of the pressure drop. Theses blow-by gases are hot, with an average temperature of 80°C, and the evaluation of the temperature variation between the inlet and outlet of the cyclone is also an important parameter.

Various numerical or experimental studies have been carried out to determine the influence of the cyclone geometrical parameters on the separation performances. Pressure drops and cut-size diameters of a wide range of cyclones can be found in the literature, together with theoretical models. Cortés et al. [1] proposed a review of these models developed for cyclone separators design. However, currently available studies on small cyclones are limited to isothermal flow conditions [2, 3]. For adiabatic wall thermal conditions, experimental [4] and numerical [5] investigations on the inlet gas temperature influence on the pressure drop and corresponding collection efficiency have been carried out.

As far as heat transfer in cyclones is concerned, currently available studies mainly focuse on the inlet velocity influence on the local or average Nusselt number [6-9], with large-size and fixed dimension cyclones. Few data are currently available for the evaluation of the heat transfer between gas and the walls, in the small cyclones range. In this experimental study, we propose an experimental determination of the total heat transfer within a small cyclone of constant diameter D=29 mm,

which corresponds to a median value of the cyclones applied to blow-by gases cleaning applications.

NOMENCLATURE

D	[m]	cyclone internal diameter
D_d	[m]	cone base diameter (« dust »)
D_H	[m]	hydraulic diameter
D_o	[m]	vortex finder internal diameter
f	[-]	friction coefficient
H	[m]	entrance height
H_{CS}	[m]	height of the control surface (model of Barth, [12])
h	[J.kg^{-1}]	specific enthalpy
K	[-]	empirical constant (model of Barth, [12])
K_A	[-]	inlet area ratio (model of Chen and Shi, [13])
L^*	[-]	dimensionless length $L^*=L_b/D$
L_b	[m]	cyclone cylinder height (« barrel »)
L_c	[m]	cyclone cone height
$\dot{m}_g$	[kg.s^{-1}]	mass flow rate
n	[-]	swirl exponent
Nu	[-]	Nusselt number
p	[Pa]	pressure
Re	[-]	Reynolds number
S	[m]	height of vortex finder
S_c	[m^2]	inner cyclone surface
S^*	[-]	dimensionless inner cyclone surface
S_f	[m^2]	inner cyclone friction surface area
T	[K]	temperature
V	[m.s^{-1}]	cross section average velocity
V_i	[m.s^{-1}]	cross section average velocity in cyclone inlet
V_o	[m.s^{-1}]	mean axial velocity in cyclone outlet
$V_{\theta CS}$	[m.s^{-1}]	internal spin velocity
$V_{\theta W}$	[m.s^{-1}]	velocity in the vicinity of the wall
W	[m]	entrance width

Special characters

α	[-]	correction coefficient of expansion loss
λ	[W.m^{-1}.K^{-1}]	gas thermal conductivity
ξ	[-]	pressure drop coefficient
μ	[kg.m^{-1}.s^{-1}]	gas dynamic viscosity
ρ	[[kg.m^{-3}]	gas density
Φ	[W]	heat transfer rate

Subscripts

b	evaluated at the bulk mean temperature
c	refers to the cooling jacket
f	evaluated at the film mean temperature
i	refers to the inlet conditions
g	refers to the gas
o	refers to the outlet conditions
w	refers to the wall conditions

EXPERIMENTAL SETUP AND METHODOLOGY

Figure 1 presents the experimental setup used in this study, which involves a hot gas flow circulating through a cyclone with an imposed temperature cold wall. A controlled air flow-rate is supplied by a compressed air unit, de-oiled, dried, and heated by a regulated electrical heater, to ensure a stable inlet gas temperature T_i, which is fixed at a constant value of 80°C.

We fixed the flow rate to values ranging from 4 to 190 Nl.min^{-1}, which is the working range of blow-by gases separators with this size. Two precision mass flow regulators with different flow ranges (40 and 200 Nl.min^{-1} full scale) have been used to adjust this flow rate.

A high flow rate of a cooling liquid is used to maintain a fixed and uniform temperature of the internal temperature of the cyclone wall. The coolant temperature is regulated via a refrigerating unit (Huber 4 kW, -55/+100°C, stability: 0.02°C). An important mixing in the external enclosure is maintained by an impeller, with strong external convective heat transfer coefficients. It was checked that under the experiments conditions, this external convective resistance, as well as the conductive resistance of the low thickness (2 mm) cyclone aluminum wall, are negligible when compared to the internal convective resistance that is being measured. During the experiments the wall temperature remained close to T_w = 10°C.

It should be noted that the entire surface exchange S_c consists of the cyclone wall, part of the inlet pipe between the T_i measurement section and the cyclone inlet, as well as part of the vortex finder, up to the outlet temperature T_o measurement point. This surface is shown in Figure 2.

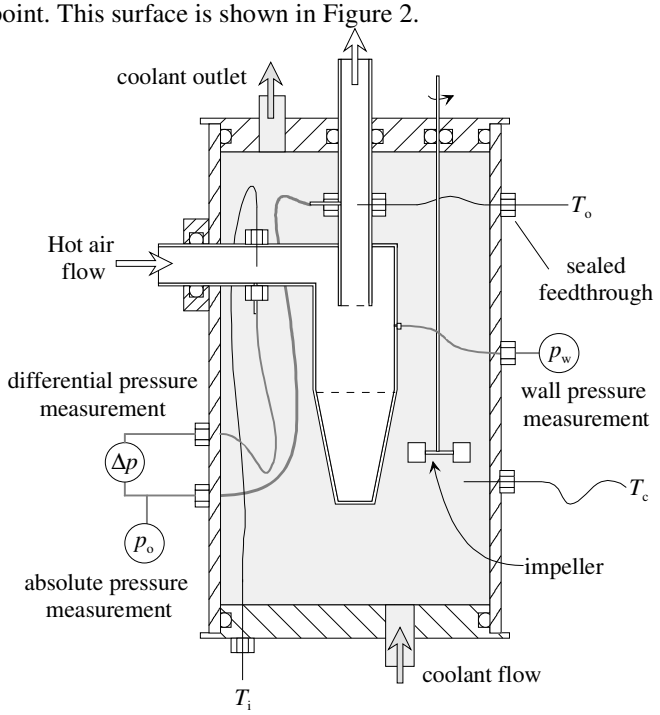

Figure 1 Schematic of the experimental setup

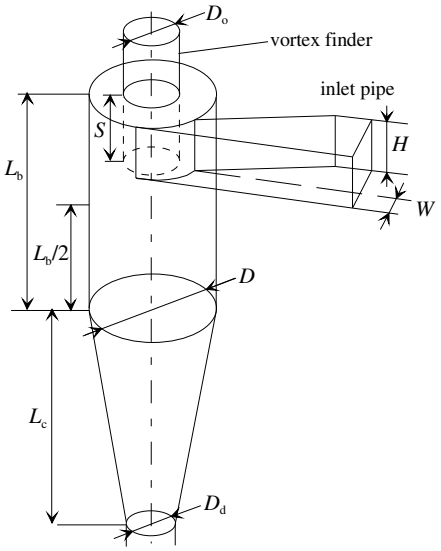

Figure 2 Cyclone geometrical parameters

In this experiment, we determined the steady heat transfer rate Φ exchanged between the gas and the cyclone by using an enthalpy balance between the inlet and outlet of the cyclone, experimentally determined with:

$$\Phi = \dot{m}_g (h_\mathrm{i} - h_\mathrm{o}) \quad (1)$$

with h_i and h_o the specific enthalpies of the gas at the inlet and outlet temperatures. The average heat transfer coefficient $\bar{h}$ between the gas and the cyclone internal wall is then defined as [10]:

$$\bar{h} = \Phi / (S_\mathrm{c}\ \Delta T_{\log}) \quad (2)$$

with S_c the internal surface of the cyclone, and $\Delta T_{\log}$ the log mean temperature difference, defined as:

$$\Delta T_{\log} = \frac{(\Delta T_\mathrm{i} - \Delta T_\mathrm{o})}{\ln(\Delta T_\mathrm{i} / \Delta T_\mathrm{o})} \quad (3)$$

where

$$\Delta T_\mathrm{i} = T_\mathrm{i} - T_\mathrm{w} \text{ and } \Delta T_\mathrm{o} = T_\mathrm{o} - T_\mathrm{w} \quad (4)$$

The average Nusselt number is then defined as:

$$\overline{Nu} = \bar{h}\ D_\mathrm{h} / \lambda_{\mathrm{g,f}} \quad (5)$$

with $\lambda_{\mathrm{g,f}}$ the gas thermal conductivity evaluated at the film mean temperature T_f = (T_b + T_w)/2, and T_b the bulk temperature T_b = (T_i + T_o)/2. D_h is the inlet hydraulic diameter, defined as:

$$D_\mathrm{h} = 2\ H\ W / (H + W) \quad (6)$$

Finally a jet Reynolds number based on the cyclone inlet conditions can be defined as:

$$\mathrm{Re}_\mathrm{i} = \frac{\rho_\mathrm{i}\ \mathrm{V}_\mathrm{i}\ D_\mathrm{h}}{\mu_\mathrm{i}} \quad (7)$$

with V_i the mass weighted average velocity in the inlet section, μ_i the gas dynamic viscosity and ρ_i its density, evaluated at the inlet temperature.

Several geometries have been tested, by varying the barrel L_b and cone L_c height. We provide the dimensions of each cyclone (see Table 1), together with the corresponding value of dimensionless inner cyclone surface at a constant temperature, defined as:

$$S^* = \frac{S_\mathrm{c}}{\pi D (L_\mathrm{b} + L_\mathrm{c})} \quad (8)$$

It should be noted that the cone height has been adjusted for every cyclone configuration, to keep L_c=L_b. The dimensionless parameter L^*=L_b/D has been varied between 0.75 and 2.5, other parameters remaining constant.

L^*	D	L_b	L_c	H	W	S	D_o	D_d	S*
0.75	29	21.75	21.75	14	6.5	18	13	11.6	1.873
1	29	29	29	14	6.5	18	13	11.6	1.612
1.25	29	36.25	36.25	14	6.5	18	13	11.6	1.458
1.5	29	43.5	43.5	14	6.5	18	13	11.6	1.355
1.75	29	50.75	50.75	14	6.5	18	13	11.6	1.282
2	29	58	58	14	6.5	18	13	11.6	1.227
2.25	29	65.25	65.25	14	6.5	18	13	11.6	1.185
2.5	29	72.5	72.5	14	6.5	18	13	11.6	1.144

Table 1 Dimensions (mm) of the tested cyclones

A scaled view of the geometry of the different cyclones is proposed in Figure 3.

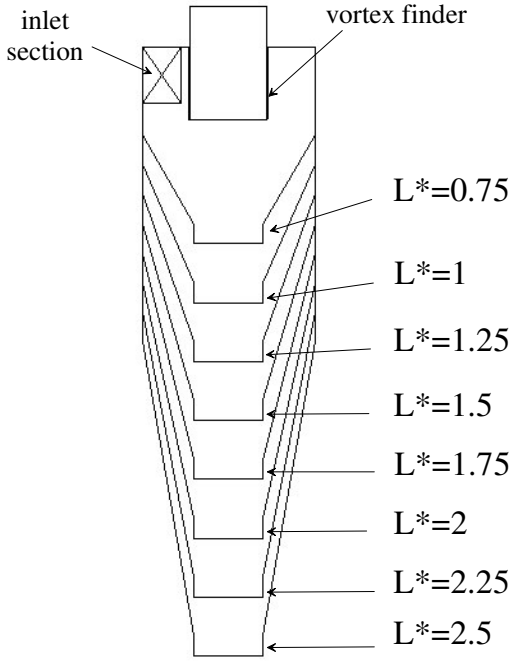

Figure 3 Scaled view geometry of the different cyclones

The pressure drop in cyclones is usually expressed as:

$$\Delta P = \xi \frac{1}{2} \rho_\mathrm{i} V_\mathrm{i}^2 \quad (9)$$

In the literature, various expressions are currently available for the evaluation of the pressure drop coefficient ξ. For most of these models, an expression of the pressure loss coefficient ξ_g for « clean » gas with no particle is proposed. The most widely used correlations for this pressure drop coefficient ξ_g are summarized in Table 2. The results obtained by application of these different models for the evaluation of ξ_g will be compared to our experimental results.

We define the ‘‘pressure drop’’ or ‘‘pressure losses’’ as the viscous dissipation of total pressure $p + 0.5\rho V^2$. However,

from an experimental point of view, it should be noted that pressure drops in cyclones are measured by the usual means of static pressure taps on the inlet and outlet duct walls [2]. In our experimental device, the determination of the pressure drop is thus based on the measurements of the static pressure at the inlet p_i and outlet p_o.

These experimental values of the static pressure must then be corrected by a dynamic pressure term, to determine the cyclone overall pressure drop:

$$\Delta P_{exp} = (p_i + 0.5\rho_i V_i^2) - (p_o + 0.5\rho_o V_o^2) \quad (10)$$

with V_i and V_o the values of the mass flow average velocity in the inlet and outlet tubes:

$$V_o = \frac{\dot{m}_g}{\rho_o S_o} \text{ and } V_i = \frac{\dot{m}_g}{\rho_i S_i} \quad (11)$$

The total pressure term in equation (10) is correctly evaluated at the inlet, as the flow is unidirectional. In the vortex finder however, a tangential velocity component persists, and the local velocity is higher than the mass flow average velocity V_o. The static pressure at the wall that is being measured is then higher than the cross-sectional static pressure average, thus leading to an underestimation of the pressure drop in the cyclone. On the other hand, the dynamic component of the total pressure due to the tangential velocity is not taken into account in equation (10), which leads to an overestimation of the pressure drop. As discussed by Cortés and Gil [1] in a review paper, there is no reason why these two effects should compensate. Cortés and Gil estimate that the uncertainty when interpreting pressure drop reports can be as high as 20%.

Model and equations

Barth (1956), [12]

$$\xi_g = (4WH/(\pi D_o^2))^2(\xi_b + \xi_o)$$

$$\xi_b = \frac{D_o}{D}\left(\frac{1}{\left(\frac{V_o}{V_{\theta CS}} - \frac{(L_b + L_c - S)}{0.5\,D_o} f\right)^2} - \left(\frac{V_{\theta CS}}{V_o}\right)^2\right), \quad f = 0.005$$

$$\xi_o = \left(\frac{v_{\theta CS}}{V_o}\right)^2 + K\left(\frac{v_{\theta CS}}{V_o}\right)^{4/3}, \text{ with } 3.41 < K < 4.4$$

$$V_o = \frac{Q_v}{\pi D_o^2/4}, \qquad V_{\theta w} = \frac{V_i R_{in}}{\alpha R}, \qquad \text{with} \qquad R_{in} = \frac{D}{2} - \frac{W}{2}$$

$$V_{\theta CS} = V_{\theta w}\frac{D/D_o}{\left[1 + \frac{H_{CS} D \pi f V_{\theta w}}{2Q_v}\right]}, \qquad \alpha = 1 - 0.4\sqrt{W/(D/2)},$$

$$H_{CS} = L_B - S + L_C\frac{D - D_o}{D - D_d}$$

Casal and Martinez (1983), [16]

$$\xi_g = 11.3\left(\frac{WH}{D_o^2}\right)^2 + 3.33$$

Dirgo (1988), [17]

$$\xi_g = 20\left(\frac{WH}{D_o^2}\right)\left[\frac{S/D}{((L_b + L_c)/D)(L_b/D)(D_d/D)}\right]^{1/3}$$

Chen and Si (2007) [13], based on Barth [12] and Muschelknautz's model [14]

$$\xi_g = \left(1 - \frac{2\alpha\tilde{W}}{1 + 1.33\tilde{W} - \tilde{D}_o}\right)^{-2} + 1.11\, f\, K_A \tilde{S}_f \tilde{v}_{\theta w}^3 \tilde{D}_o^{-1.5n} + \frac{\tilde{v}_{\theta w}^2}{(\tilde{r}_c \tilde{D}_o)^n} + \frac{1}{K_A^2(\tilde{D}_o^2 - \tilde{r}_c^2)^2}$$

$$K_A = \frac{\pi D^2}{4WH}, \ \tilde{W} = W/D, \ \tilde{D}_o = D_o/D, \ \tilde{v}_{\theta w} = \frac{v_{\theta w}}{V_i}$$

$$\tilde{S}_f = \frac{S_f}{\pi D^2/4}, \ \tilde{v}_{\theta w} = \frac{1.11 K_A^{-0.21}\tilde{D}_o^{0.16}\,\mathrm{Re}_o^{0.06}}{1 + f\,\tilde{S}_f\sqrt{K_A \tilde{D}_o}}, \ \mathrm{Re}_o = \frac{\rho_g V_i D}{\mu_g K_A \tilde{D}_o}$$

$$\tilde{r}_c = 0.38\tilde{D}_o + 0.5\tilde{D}_o^2, \ n = 1 - \exp\left[-0.26\,\mathrm{Re}_o^{0.12}\left(\frac{S - H}{W}\right)^{-0.5}\right]$$

$$S_f = \pi\left[\frac{(D^2 - D_o^2)}{4} + (DL_b + D_o S) + \frac{(D + D_d)}{2}\sqrt{L_c^2 + \frac{(D - D_d)^2}{4}}\right]$$

$$\alpha = \frac{1}{\chi}\left\{1 - \sqrt{1 + 4\left[\left(\frac{\chi}{2}\right)^2 - \frac{\chi}{2}\right]\sqrt{1 - (1 - \chi^2)(2\chi - \chi^2)}}\right\} \text{ with } \chi = W/(0.5D)$$

Table 2 Analytical models for the evaluation of the pressure drop coefficient ξ_g in cyclones

PRESSURES LOSSES EXPERIMENTAL RESULTS

In Figure 4, we present a comparison between the experimental determinations of pressure losses, together with the results obtained by using the models presented in Table 2, for the cyclone configuration with L^*=2 (see Table 1).

For this particular value L^*=2, we can see that a very good agreement is obtained between our measurements and the pressure losses evaluated with Chen and Shi's model [13], on the entire flow range. This result is conforming to the conclusions of Hsiao *et al.*[15], who found out that the Chen and Shi and Dirgo's models were the most relevant in their confrontation between models and measurements.

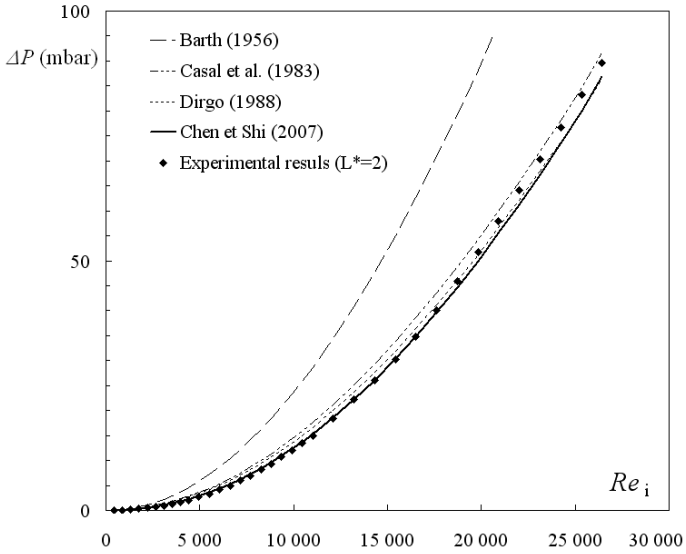

Figure 4 Pressure losses: comparison between experimental determinations and models (L^*=2)

As illustrated in Figure 5, the agreement between the Chen and Shi's model and the measurements is still very good for L^*=1.

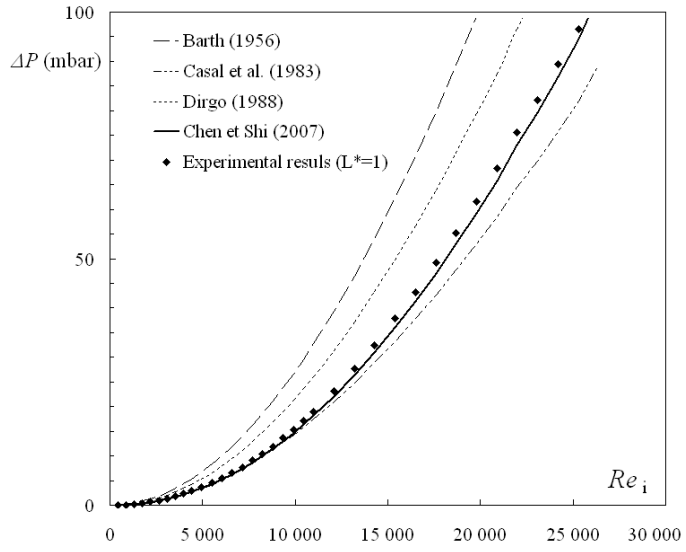

Figure 5 Pressure losses: comparison between experimental determinations and models (L^*=1)

However, when decreasing the cyclone height to L^*=0.75, we observe that the Chen and Shi model disagrees with the experimental data, as illustrated in Figure 6.

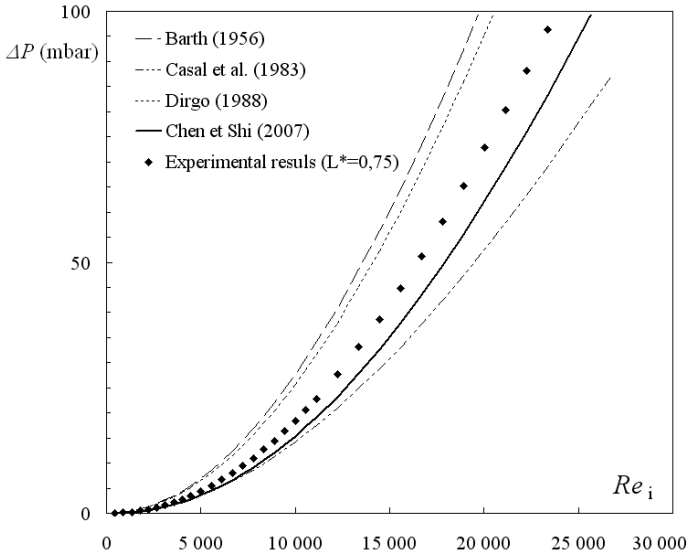

Figure 6 Pressure losses: comparison between experimental determinations and models (L^*=0.75)

We present in Figure 7 measurements of the pressure drop coefficient ξ_g as a function of the dimensionless parameter L^*, and for a fixed value of the Reynolds number Re_i=10 000. These results are presented with the corresponding values of ξ_g obtained by application of the models from the literature, and we can see that the values of the pressure drop coefficient as predicted by Barth [12] and Casal's models [16] are constant, while the models proposed by Dirgo [17] and Chen and Shi [13] are predicting a decrease of the ξ_g when increasing L^*. For this fixed value of the Reynolds number Re_i=15 000, the model by Chen and Shi is the only one to provide good agreement with our measurements. As we can notice, the model does not predict correctly the pressure lost coefficient, for the lowest value L^*=0.75.

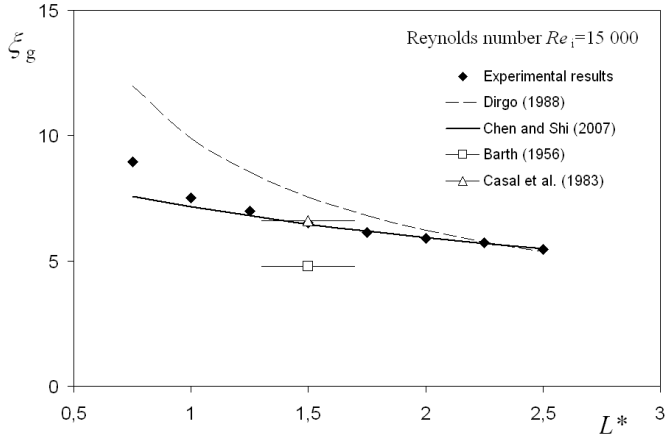

Figure 7 Pressure losses coefficient ξ_g : comparison between experimental determinations and models, as a function of L^* (Re_i=15 000)

We report in Figure 8 the corresponding comparison between our experimental determinations of ξ_g and results obtained by using the models proposed by Dirgo [17] and Chen and Shi [13], for three values of the Reynolds number.

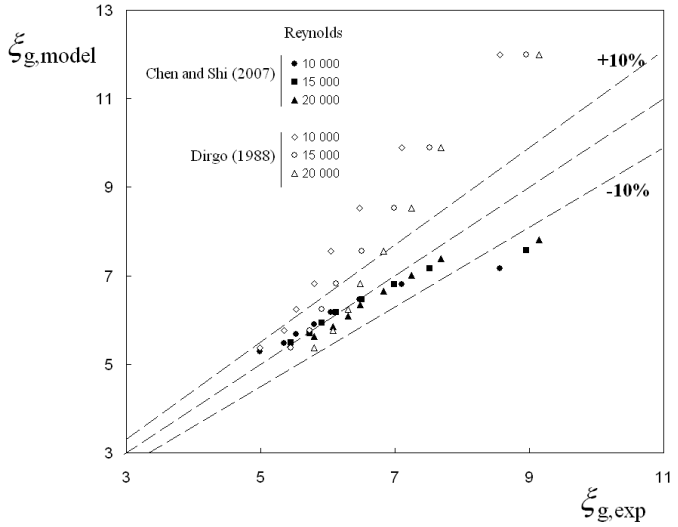

Figure 8 Pressure losses coefficients: comparison between experimental determinations and models (0.75< L*<2.50)

The Chen and Shi model appears to be the most relevant for the determination of the pressure drop coefficient ξ_g. The agreement between the model and measurements is very good, expect for the L*=0.75. If we consider a restricted range for the cyclone height 1 < L* < 2.5, the maximum deviation between measurements and Chen and Shi's model is lower than 10%, for inlet Reynolds number values in the range 10 000 to 20 000.

HEAT TRANSFER EXPERIMENTAL RESULTS

For the average Nusselt numbers $\overline{Nu}$ determination, we use the experimental setup described previously (Figure 1). This experimental procedure, though not leading to the local heat flux determination, permits the determination of the average wall heat transfer coefficient, by the simultaneous measurements of T_i, T_o, T_w and mass flow rate. The convective heat flux has been experimentally determined using equation (1). The experimental average Nusselt number was then determined by using equation (5), with the gas thermal conductivity λ_g being evaluated at the bulk gas temperature $T_b = (T_i + T_o)/2$.

Experimental results were obtained for various values of L*, with $0.75 \le L^* \le 2.5$, and for inlet Reynolds number Re_i in the range $400 \le Re_i \le 20\,000$. The uncertainty on the average Nusselt number $\overline{Nu}$ due to errors on temperature measurements, mass flow measurements, and thermal losses has been investigated.

The heat transfer experiments reported here were repeated between three and ten times, depending on the relative standard deviation of the experimental results. All the measured values were within 5% of the average value.

Figure 9 shows the variation of the average Nusselt number $\overline{Nu}$ with the inlet Reynolds number Re_i, for 0.75 < L* < 2.5.

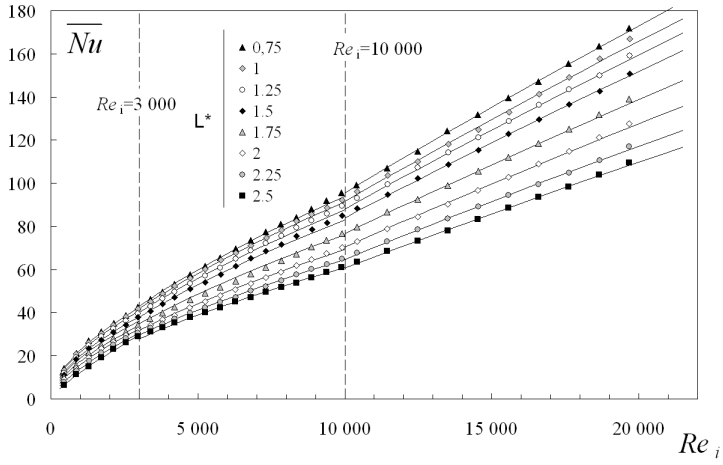

Figure 9 Experimental average Nusselt number as a function of the inlet Reynolds number, for 0.75< L*<2.50

Three Reynolds ranges can be observed, which correspond to the laminar regime, transitional and fully turbulent flow regime. The Reynolds number limits have been considered as Re_i=3000 and Re_i =10 000. The upper limit Re_i =10 000 is a classical value that is currently being used for pipe flow heat transfer correlations [19], while the lower limit is also a typical value for the laminar flow Reynolds number limit.

CORRELATION

For the evaluation of heat transfer rate, the log mean temperature difference (LMTD) method is conventionally used to calculate the total convective thermal flux [10, 18], in heat exchangers:

$$\Phi = \bar{h}\, S_c\, \Delta T_{log} \tag{12}$$

with S_c the internal surface at a constant temperature between the inlet and outlet temperature measurement points, and ΔT_{log} the log mean temperature difference (see Eq. (3)). The average Nusselt number is then usually expressed as a function of the inlet Reynolds and Prandtl numbers, in the form:

$$\overline{Nu} = A\, Re_i^m\, Pr^n \tag{13}$$

For gas cooling application, the value of the Prandtl number exponent n is usually considered as n=0.3 [10, 18]. The values of the A and m set of coefficient were obtained, by least squares method of all experimental results measured for varied Reynolds numbers and values of the L* parameter, with this fixed value of the Prandtl number exponent n=0.3.

Three flow regime have been identified: for Reynolds number values Re_i lower than 3000, we have a laminar flow regime, with given values of A and m coefficients. For Reynolds values Re_i in the range 3000 to 10 000, a second set of coefficients is proposed, corresponding to the transition

regime. For Reynolds number Re_i in the range $10000 < \mathrm{Re_i} < 20000$, we have a fully turbulent flow, with a third set of coefficients.

The average relative deviation of the experimental values to this correlation is 1.1%, with a maximum deviation of 5%, on the whole range of Reynolds number.

	A		
L*	$\mathrm{Re_i} < 3000$	$3000 < \mathrm{Re_i} < 10000$	$10000 < \mathrm{Re_i} < 20000$
0.75	0.491	0.263	0.040
1	0.472	0.255	0.038
1.25	0.415	0.245	0.037
1.5	0.361	0.232	0.035
1.75	0.287	0.213	0.032
2	0.204	0.194	0.030
2.25	0.121	0.181	0.027
2.5	0.057	0.170	0.025

	m		
L*	$\mathrm{Re_i} < 3000$	$3000 < \mathrm{Re_i} < 10000$	$10000 < \mathrm{Re_i} < 20000$
0.75	0.570	0.65	0.85
1	0.570		
1.25	0.577		
1.5	0.589		
1.75	0.610		
2	0.647		
2.25	0.704		
2.5	0.793		

Table 3 Correlation coefficients, for the different inlet Reynolds number ranges, and different values of the *L** parameter

CONCLUSION

The gas-to-wall heat transfer for a flow in a constant wall temperature cyclone configuration has been investigated. Experimental measurements were used to derive an average Nusselt number correlation in the cyclone inlet Reynolds number range $400 \leq Re_i \leq 20\,000$ and for various geometrical parameters $0.75 \leq L^* \leq 2.5$. Static pressure measurements at the inlet and outlet of the cyclone have been used to evaluate the pressure drop in the cyclone, and a comparison between these results has been carried out. The conclusions of the analysis can be summarized as follows:

1. This experimental study confirm the model proposed by Chen and Shi is particularly relevant for the evaluation of the pressure losses in this range of small cyclones, except for values of L* lower than one.

2. An average Nusselt number correlation has been proposed. This correlation (13) is thought to be applicable in many engineering configurations requiring the evaluation of the temperature variation in small cyclones.

REFERENCES

[1] Cortés C., and Gil A., Modeling the gas and particle flow inside cyclone separators, *Progress in Energy and Combustion Science*, 33 (2007), 409-452.

[2] Zhu Y., and Lee K. W., Experimental study on small cyclones at high flowrates, *Journal of aerosol Science*, 30 (1999), 1303-1315.

[3] Ma L., Ingham D. B., and Wen X., Numerical modelling of the fluid and particle penetration through small sampling cyclones, *Journal of aerosol Science*, 31 (2000), 1097-1119.

[4] Bohnet M., Influence of the gas temperature on the separation efficiency of aerocyclones, *Chemical Engineering and Processing*, 34 (1995), 151-156.

[5] Gimbun J., Chuah T. G., Fakhru'l-Razi A., and Choong, T.S.Y., The influence of temperature and inlet velocity on cyclone pressure drop: a CFD study, *Chemical Engineering and Processing*, 44 (2005), 7-12.

[6] Karagoz I., and Kaya F., CFD investigation of the flow and heat transfer characteristics in a tangential inlet cyclone, *International Communications in Heat and Mass Transfer*, 34 (2007), 1119-1126.

[7] Gupta A. V. S. S. K. S, and Nag P. K., Prediction of heat transfer coefficient in the cyclone separator of a CFB, *International Journal of Energy Ressearch*, 24 (2000), 1065-1079.

[8] Lédé J., Li H. Z., Soulignac F., and Villermaux J., Le cyclone réacteur III : mesure de l'efficacité des transferts de chaleur et de matière entre les parois et un gaz circulant seul, *The Chemical Engineering Journal*, 45 (1990), 9-24.

[9] Szekely J., and Carr R., Heat transfer in a cyclone, *Chemical Engineering Science*, 21 (1966), 1119-1132.

[10] Whitaker J. A., Fundamental Principles of Heat Transfer. Pergamon Press, New York, (1977).

[11] Incropera F. P., De Witt D. P., and Lavine A. S., Fundamentals of Heat and Mass Transfer. 6th ed., Wiley, New York, (2007) 514-518.

[12] Barth W., Berechnung und Auslegung von Zyklonabscheidern auf Grund neuerer Untersuchungen, *Brennst-Waerme-Kraft*, 8 (1956), 1-9.

[13] Chen J., and Shi M., A universal model to calculate cyclone pressure drop, *Powder Technology*, 171 (2007), 184-191.

[14] Muschelknautz E., and Kambrock W., Aerodynamische Beiwerte des Zyclonabscheiders aufgrund neuer und verbes-serter Messungen, *Chemie Ingenieur Technik*, 42 (1970), 247–255.

[15] Hsiao T., Chen D., and Son S.Y., Development of mini-cyclones as the size-selective inlet of miniature particle detectors, *Journal of Aerosol Science*, 40 (2009), 481–491.

[16] Casal J., and Martinez-Benet J.M., A better way to calculate cyclone pressure drop, *Chemical Engineering*, 90 (1983), 99–100.

[17] Dirgo J. A., Relationships Between Cyclone Dimensions and Performance. Ph.D. Thesis, Harvard University : Cambridge, MA, (1988).

[18] Lienhard IV J. H., and Lienhard V, J. H, A heat transfer textbook. Cambridge (Massachusetts): Phlogiston Press, (2003).

[19] Kakaç S., and Yener Y., Convective Heat transfer. CRC Press, Boca Raton (Florida), (1995).